

Electromechanical Emulation of Hydrokinetic Generators for Renewable Energy Research

Jason C. Neely, *Member, IEEE*, Kelley M. Ruehl, Richard A. Jepsen, Jesse D. Roberts, Steven F. Glover, *Senior Member, IEEE*, Forest E. White, *Member, IEEE*, Michael L. Horry

Abstract—The pace of research and development efforts to integrate renewable power sources into modern electric utilities continues to increase. These efforts are motivated by a desire for cleaner, cheaper and more diverse sources of energy. As new analyses and controls approaches are developed to manage renewable sources and tie them into the grid, the need for these controls to be tested in hardware becomes paramount. In particular, hydrokinetic power is appealing due to its high energy density and superior forecastability; however, its development has lagged behind that of wind and solar due in part to the difficulty of acquiring hardware results on an integrated system. Thus, as an alternative to constructing an elaborate wave-tank or locating a power lab riverside, this paper presents a method based on electromechanical emulation of the energy source using a commercially available induction motor drive. Using an electromechanical emulator provides an option for universities and other laboratories to expand their research on hydrokinetics in a typical laboratory setting.

Index Terms—Marine hydrokinetics, renewable energy, river turbine, wave energy converter, point absorbers

I. INTRODUCTION

THE modern electric utility is the product of over a hundred years of development and evolution, optimized primarily for fossil-fuel based dispatchable generation. However, for both economic and environmental reasons, the grid is quickly evolving to incorporate renewable energy sources and mitigate fossil fuel consumption. This has led to several nations legislating greater renewable integration including the EU 20/20/2020 plan and similar 20 percent by 2020 targets set by Egypt, Australia and a majority of states in the United States (US) [1], [2]. In fact, some US states have committed to even more aggressive measures such as House Bill 306 wherein Alaska has committed itself to achieve 50 percent renewable / alternative energy by 2025 [2]. To meet these objectives, it is important to consider all available renewable sources. Hydrokinetic energy sources have been particularly interesting due to the high power density of river and tidal water currents as well as ocean waves that have excellent forecastability [3]. In Alaska for example, some of the coast line has potentially 40-60 kW per meter crest length of available power density [3].

Unlike dispatchable generation, a significant issue with renewable sources of energy is variability and intermittency. These effects may be mitigated through diversification of the

renewable profile, integration of sources from geographically separated regions, incorporation of energy storage, demand side management, or advanced communication and controls. To investigate these options further, Sandia National Laboratories is expanding their renewable energy research to develop new tools for the design and analysis of power systems with high penetration levels of stochastic renewable sources. A necessary step for this research is experimental validation, which has resulted in the development of a hardware testbed called the Secure Scalable Microgrid Testbed (SSMTB) [4], [5], [6]. Given a time-indexed weather profile (i.e. wind speed (m/sec), wave crest (m), river currents (m/sec), solar irradiance (W/m^2), etc.) as well as a load profile (W or Ω), the testbed can be used to repeat an experiment over and over using different control schemes but the same simulated weather pattern. This is done from a central computer interface. The lab and the interface can be seen in Figure 1.

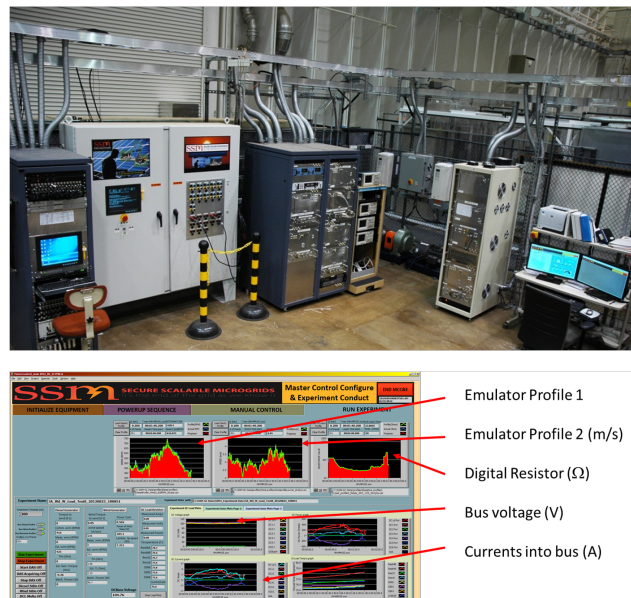


Fig. 1. Photo of Secure Scalable Microgrid Testbed and Master Control Interface

Marine Hydrokinetic (MHK) devices are a nascent renewable technology, with great potential to help us meet our growing energy needs. They benefit from converting energy into usable power from highly dense energy resources, including: river, tidal and ocean currents, and ocean waves. In this paper, a simple method for incorporating hydrokinetic sources into the SSMTB for laboratory experiments is presented,

Sandia National Laboratories, Albuquerque, NM, 87123 e-mail: jneely@sandia.gov.

F. White is with SAIC, 2109 Air Park Rd SE, Albuquerque, NM 87106

Manuscript received July 31st, 2013

including the emulation of a dual-rotor river cross-flow turbine and a point absorber wave energy converter (WEC) [7], [8]. Given a hydrokinetic reference model developed using careful analysis, field data and/or wave-tank experiments, the emulator allows the development of control schemes and algorithms that tie the hydrokinetic source into a larger power system including: development of maximum power point tracking methods, integration with off-shore wind, shadowing effects, phase-control of point-absorbers, or incorporation of energy storage.

In section II, the hydrokinetic dynamic models for a river turbine and a point absorber used in this study are presented. In section III, the hydrokinetic emulator is described, including analysis and a hardware description. In section IV, system parameters are given for a river turbine and both simulation and experimental results are presented. In section V, simulation and experimental results are given for a point absorber. Finally, conclusions and future work are discussed in section VI.

II. HYDROKINETIC DYNAMIC MODELS

In this section, the dynamic models of two very different hydrokinetic generators are described, and a model is presented for each.

A. River Turbine Model

For a river turbine, the mechanical power delivered to the rotor is given by

$$P_{turb} = \frac{1}{2} C_p(\lambda) \rho_w A_r v_w^3 \quad (1)$$

where $C_p(\lambda)$ is the power coefficient, ρ_w is the density of water, A_r is the cross-sectional area of the rotor, and v_w is the velocity of the water current, and λ is the ratio of the water velocity and the velocity of the rotor tip speed, $\lambda = (R_{turb}\omega_{turb})/v_w$, where R_{turb} is the rotor radius in meters [9]. Thus, for a mechanical rotor speed of ω_{turb} , the mechanical torque delivered to the rotor by the water flow is given by

$$T_{turb} = \frac{P_{turb}}{\omega_{turb}} = \frac{1}{2\omega_{turb}} C_p(\lambda) \rho_w A_r v_w^3 \quad (2)$$

The dynamic response of the turbine will depend on the torque delivered by the cross-flow of water (2) as well as the torque of the power take off generator, the shaft and gearbox losses and the system inertia. The turbine velocity dynamic is thus modeled as the following

$$\frac{d\omega_{turb}}{dt} = \frac{T_{turb} - N_{gb}T_{pto} - B_{gb}\omega_{turb}}{J_{turb} + N_{gb}^2 J_{pto}} \quad (3)$$

where N_{gb} is the gearbox ratio such that $\omega_{pto} = N_{gb}\omega_{turb}$ where ω_{pto} is the rotational speed of the power take-off generator, T_{pto} is the power take-off generator torque, B_{gb} is the damping coefficient of the gearbox, and J_{turb} and J_{pto} are the moments of inertia of the turbine and power take-off generator respectively. As will be seen in the next section, however, it is convenient to represent the dynamics in terms of the power take-off generator rotation rather than turbine rotation. By substituting $\omega_{pto} = N_{gb}\omega_{turb}$ into equation

(3), the generator dynamic equation may be written as the following.

$$\frac{d\omega_{pto}}{dt} = \frac{(1/N_{gb})T_{turb} - T_{pto} - (1/N_{gb}^2)B_{gb}\omega_{pto}}{(1/N_{gb}^2)J_{turb} + J_{pto}} \quad (4)$$

B. Point Absorber Model

For a monochromatic wave, the wave power is given by

$$P_{wave} = \frac{\rho_{sw} g^2 H^2 T}{32\pi} CW \quad (5)$$

where ρ_{sw} is the density of seawater, g is the gravitational constant, H is the wave height (m), T is the wave period (sec), and CW is the WECs capture width (m) [3]. In this paper, the focus is on the single-body point absorber, which extracts power from the waves using a single mass that moves with changes in seawater level; the system is depicted in Figure 2.

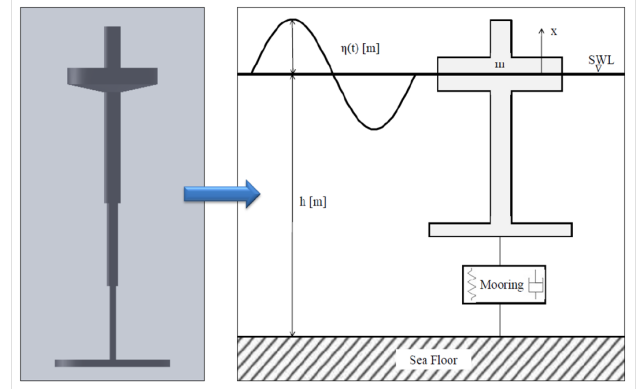


Fig. 2. Illustration of Single-Body Point Absorber (reproduced from [8])

The single-body point absorber equation of motion with power take-off is based on the Cummins' time domain impulse response model for ship motions [8] and given as

$$F_e(t) - F_r(t) - F_m(x, \dot{x}) = K_{hs}x + B_{pto}\dot{x} + (m + A(\infty))\ddot{x} \quad (6)$$

where $F_e(t)$ is the excitation force given by

$$F_e(t) = \int_{-\infty}^{\infty} \eta(\tau) f_e(t - \tau) d\tau \quad (7)$$

$F_r(t)$ is the radiation force given by

$$F_r(t) = \int_{-\infty}^t f_r(t - \tau) \dot{x} d\tau \quad (8)$$

F_m is the mooring force given by

$$F_m(t) = 8k_m \left(1 - \frac{l_m}{(l_m^2 + x^2)^{1/2}} \right) x \quad (9)$$

K_{hs} is a hydrostatic force constant given by

$$K_{hs} = \rho_{sw} g A \quad (10)$$

B_{pto} is a viscous damping term associated with the power take off resulting in a mechanical power take off of $P_{pto} = B_{pto}\dot{x}^2$ in Watts, m is the mass of the buoy and $A(\infty)$ is the equivalent

added mass of the sea water. It is noted that equation (6) resembles a classic mass-damper system except that the force calculations are considerably more complex. Equations (7) and (8) are based on computation of an impulse response function. In particular, equation (7) is *noncausal*, that is the computation requires information about future values of wave height $\eta(t)$.

In the next section, the emulator hardware will be presented. The emulator hardware consists of a rotational motor-generator system, a simple method of translating the power take-off of the linear up and down motion of the point absorber into rotational generation is developed.

III. HYDROKINETIC EMULATOR

In this section, details of the hydrokinetic emulator are given, including hardware realization and controls.

A. Emulator Hardware

The hydrokinetic emulator is similar in construction to the diesel engine emulator described in [4]. It consists of an 11.2 kW Baldor induction motor with ABB ACS800 motor drive system. The motor includes a speed encoder which enables the ABB drive to implement a Direct Torque Control (DTC) that realizes a commanded torque with an accuracy of 1% within 5 msec of reading the register.

Control is done onboard a National Instrument (NI) 3110 industrial computer. The NI 3110 communicates with the ABB drive using Modbus/TCP commands. Specifically, the NI 3110 runs a LabVIEW development environment that includes the Mathscript RT toolkit. The discrete-time controls are written in Matlab and implemented within a LabVIEW shell on the NI 3110 [10], [11]. Measured speed encoder values are read from the ABB drive and new torque commands are sent to the ABB drive each 24 msec sampling period. The emulator hardware is depicted in Figure 3.

The Baldor motor drives a Georator 36-013-1 10-kVA permanent-magnet generator with a rated speed of 1714 RPM. For both the river turbine and the point-absorber, the Georator, with appropriately selected scale factors, will be used to represent their respective power take-off systems.

B. Emulator Dynamics and Controls

The dynamic equation for the emulator is given simply as follows

$$\frac{d\omega_{em}}{dt} = \frac{T_{im} - B_{em}\omega_{em} - T_{gen}}{J_{em}} \quad (11)$$

where ω_{em} is the rotor speed for the induction motor and generator in radians/second, T_{im} is the induction motor torque, B_{em} is the damping coefficient of the emulator, T_{gen} is the torque of the emulator generator and J_{em} is the moment of inertia of the assembly.

The emulator base speed and power ratings are available as nameplate values. The emulator inertia and damping coefficient were determined from experiment. Specifically, the induction motor torque was stepped, and the inertia and damping coefficient were determined from the rise time and steady state value of the rotor speed. Finally, a scale factor k_{sc}

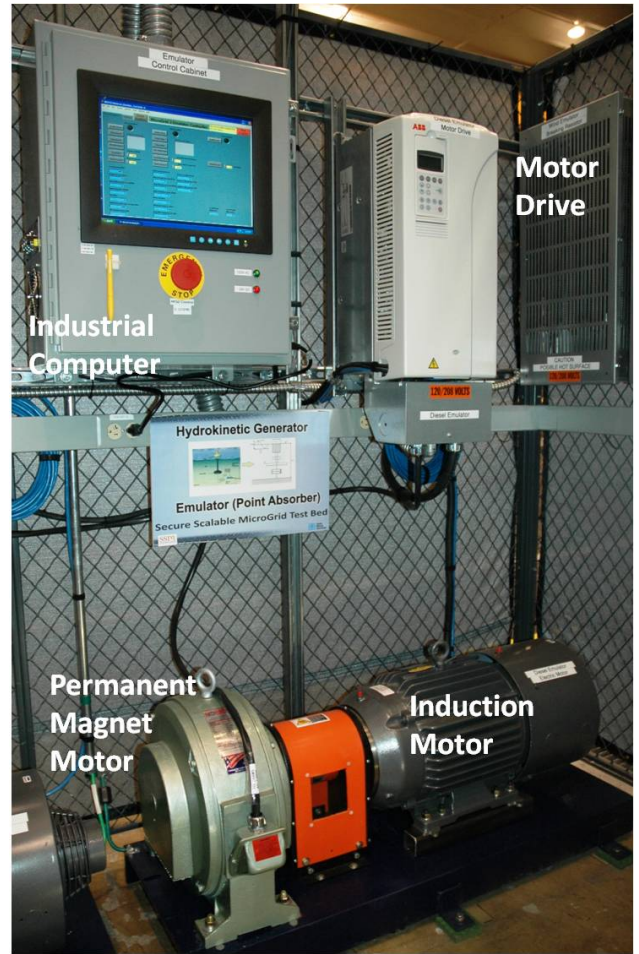


Fig. 3. Emulator Hardware and Georator 10-kVA permanent magnet generator

is included as the ratio of the base power of the laboratory emulator to the physical system being emulated. The scale factor k_{sc} scales the inertia, damping coefficient and turbine torque equally, thus preserving the time constant of the initial system.

C. Generator Torque Estimator

The emulator rotor speed ω_{em} is measured using a speed encoder and the induction motor torque T_{IM} is commanded by the control, but the generator torque is not measured. As will be shown, a value for the generator torque is necessary for proper operation of the emulator; thus, an estimator is developed. Approximating T_{gen} as constant ($\frac{d}{dt}T_{gen} = 0$), the estimator dynamics are given as

$$\frac{d}{dt} \begin{pmatrix} \hat{\omega}_{em} \\ \hat{T}_{gen} \end{pmatrix} = \begin{pmatrix} \frac{-B_{em}}{J_{em}} & \frac{-1}{J_{em}} \\ 0 & 0 \end{pmatrix} \begin{pmatrix} \hat{\omega}_{em} \\ \hat{T}_{gen} \end{pmatrix} + \begin{pmatrix} \frac{1}{J_{em}} \\ 0 \end{pmatrix} T_{im} + \begin{pmatrix} \kappa_{\omega} \\ \kappa_T \end{pmatrix} \Delta\omega_{em} \quad (12)$$

where \hat{T}_{gen} and $\hat{\omega}_{em}$ are estimated quantities, $\Delta\omega_{em} = (\hat{\omega}_{em} - \omega_{em})$ is the speed error, and $\kappa_{\omega}, \kappa_T$ are estimator gains. A more complete explanation of how to choose these

estimator parameters and implement the estimator in discrete-time is given in [4], [5].

The emulator and estimator parameters used herein are summarized in Table I.

TABLE I
EMULATOR PARAMETERS

Description	Parameter	Value	Units
Emulator Base Power	$P_{B,em}$	10.0	kW
Emulator Inertia	J_{em}	0.4005	kg·m ²
Emulator Damping Coeff.	B_{em}	0.0174	Nm·sec/rad
Speed estimator gain	κ_ω	-20.0	1/sec
Torque estimator gain	κ_T	40.01	Nm/rad

D. River Turbine Emulator Control

To emulate the river turbine dynamics, the following equalities are established

$$\omega_{em} = \left(\frac{n_{em}}{n_{pto}} \right) \omega_{pto} \quad (13)$$

$$T_{gen} = \left(\frac{n_{pto}}{n_{em}} \right) T_{pto} \quad (14)$$

where n_{pto} is the base speed of the power take-off generator on the physical river turbine and n_{em} is a nominal emulator generator speed computed using the maximum desired emulator speed, maximum flow rate (computed from (1) and rated power), turbine radius and the optimal tip speed ratio as shown in equation (15).

$$n_{em} = \frac{n_{pto} R_{turb} \max(\omega_{em})}{N_{gb} \lambda^* \max(v_w)} \quad (15)$$

Equations (4)-(14) are combined, and the following is computed for the commanded induction motor torque after some algebra

$$\begin{aligned} T_{im}^* = & \left(\frac{n_{em}}{n_{pto}} \cdot \frac{(1/N_{gb})J_{em}}{(1/N_{gb}^2)J_{turb} + J_{pto}} \right) T_{turb} \\ & + \left(1 - \left(\frac{n_{em}}{n_{pto}} \right)^2 \frac{J_{em}}{k_{sc} \left((1/N_{gb}^2)J_{turb} + J_{pto} \right)} \right) T_{gen} \\ & + \left(B_{em} - \frac{(1/N_{gb}^2)B_{gb}J_{em}}{(1/N_{gb}^2)J_{turb} + J_{pto}} \right) \omega_{em} \end{aligned} \quad (16)$$

For the emulator, a discrete-time version of equation (16) with parameter values developed from [7] is developed and used directly to compute turbine power and thus turbine torque in the Reference Model 2 (RM2) river turbine. For the point absorber, the emulator uses a more sophisticated model of a single mass system with power take-off, based on the analysis in [8]. In each, the emulator is connected at the shaft to a 3- Φ permanent magnet generator. For the river turbine, the system is tested with the generator connected to a simple 3- Φ wye-connected resistive load; for the point absorber, the generator is connected to a DC bus through a rectifier.

E. Point Absorber Emulator Control

The third order dynamics of the single-body point absorber may be represented conveniently by three ordinary differential equations. Identifying the velocity and acceleration of the mass as $v_m = \dot{x}$ and $a_m = \ddot{x}$, the dynamics may be written as

$$\frac{d}{dt} a_m = \frac{1}{m + A(\infty)} (-B_{pto} v_m - K_{hs} x + F_e - F_r - F_m) \quad (17)$$

$$\frac{d}{dt} v_m = a_m \quad (18)$$

$$\frac{d}{dt} x = v_m \quad (19)$$

Discrete-time equivalents are developed for equations (17)-(19), and the buoy velocity v_m and position x are solved using trapezoidal integration. Although the buoy exhibits linear oscillatory behaviour, the power take-off can be realized using rotational generation. For example, in [8], a detailed model is presented for a hydraulic motor-generator system. For the system presented herein, however, an idealized model is considered that preserves the power balance $B_{pto} v_m^2 = T_{im} \omega_{em}$ while neglecting the dynamics of the power take-off. Specifically, the emulator induction motor torque command used herein is simply

$$T_{im}^* = k_{sc} \frac{B_{pto} v_m^2}{\omega_{em} + \epsilon} \quad (20)$$

where ϵ is included to avoid a divide by zero and k_{sc} is again used to scale down power levels. The point absorber x position and velocity will be tracked numerically and the output power realized using equation (20). It is noted from (20) that the torque is always positive and that the generator will rotate in one direction.

In the emulator software, the excitation and radiation forces are computed using LabVIEW's point-by-point Finite impulse response filter. The forces are then summed and input into the Matlab environment buried therein where the buoy position, velocity and emulator torque are computed.

IV. SIMULATION AND HARDWARE RESULTS FOR RIVER TURBINE EMULATOR

In this section, parameters for a physical river turbine system will be identified, and its performance will be compared to that of the emulator in simulation. The emulator will then be demonstrated in hardware.

A. River Turbine Description

The river turbine emulated in this study is based on the Reference Model 2, Cross-Flow River Turbine presented in [7]. Therein, the system includes two rotors, each rated for 50 kW of generation and connected to a dedicated generator through a gearbox. See Figure 4.

The rotor inertia was estimated using the total mass of the rotor with the assumption that the struts and blades had the same linear density. The damping coefficient was estimated by attributing all inefficiencies of the Rexnord Planet Gear 7000, Titan Plus gearbox to the term $\omega_{turb}^2 B_{gb}$ at the gearbox's full power and full speed.

The power coefficient was determined by performing a detailed CACTUS simulation at several values for tip-speed ratio. CACTUS (Code for the Analysis of Cross- and axial-flow Turbine Simulation) is "... an improved version of the original VDART3 code, which was developed during the Sandia National Laboratories VAWT research program" [7]. With 20 points computed for $\lambda, C_P(\lambda)$, the data was fit to a 4th order polynomial using the Matlab function *polyfit*. This polynomial was then used by the emulator to establish C_P . See Figure 5.

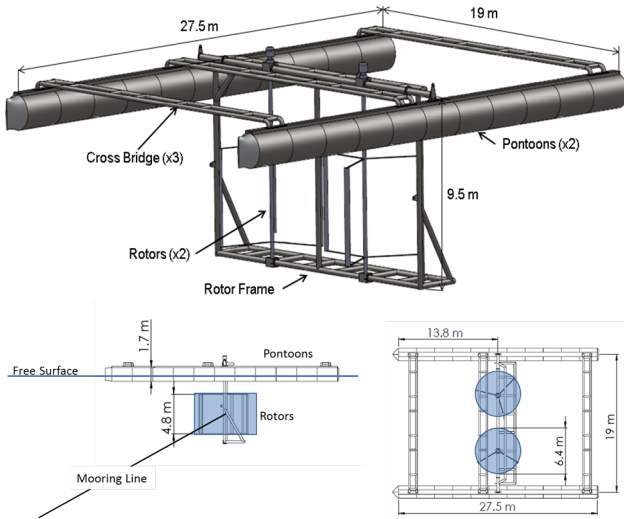


Fig. 4. Illustration of River Turbine (reproduced from [7])

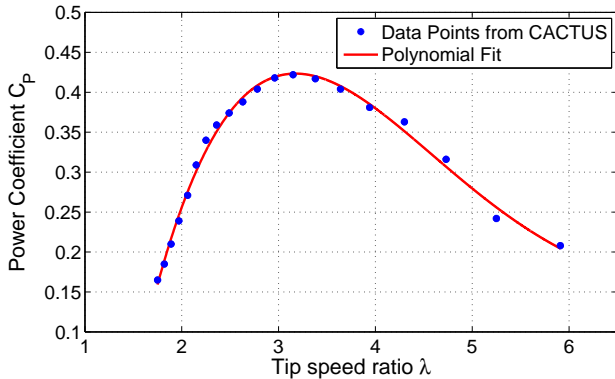


Fig. 5. Rotor Turbine Power Curve

Since the emulator hardware is limited to 10 kW however, the 50 kW rotor parameters were scaled down by 0.2. Specifically, to preserve the system time constant, system power, inertia and damping were each scaled together. The resulting system represents the dynamic performance of a turbine with diameter 6.45 meters but a blade height of only 0.97 meters and a gearbox and generator reduced in size accordingly.

In simulation and in hardware, the permanent magnet generator is connected to a 3-phase wye connected resistive load. The system is illustrated in Figure 6. The turbine, load and emulator parameters used in this study are given in Table II.

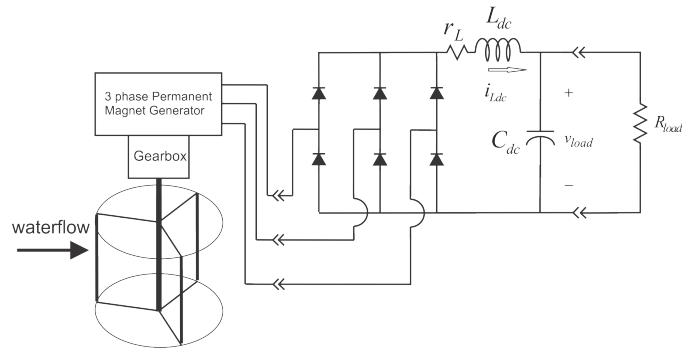


Fig. 6. Schematic representation of river turbine with rectifier and electrical load

TABLE II
RIVER TURBINE EMULATOR EXPERIMENT PARAMETERS

Description	Parameter	Value	Units
Turbine rated power	$P_{B,turb}$	50.0	kW
Turbine moment of inertia	J_{turb}	6911	kg·m ²
Gearbox damping	B_{gb}	37.26	Nm·sec/rad
Gearbox ratio	N_{gb}	13.85	unitless
Power Take off inertia	J_{pto}	7.80	kg·m ²
Power Take off rated speed	n_{pto}	146	RPM
Emulator power scale factor	k_{sc}	0.2	unitless
Emulator nominal speed	n_{em}	863.1	RPM
Optimal Tip-speed ratio	λ^*	3.15	unitless
Maximum flow rate considered	$max(v_w)$	1.9633	m/sec
Load Phase resistance	R_{load}	12.5	Ω

Both static and dynamic tests were performed to compare the hardware performance with expected response. In the first test, the steady state electrical output power was measured for several water velocities between 0.7 m/sec and 1.1 m/sec in steps of 0.05 m/sec. The turbine mechanical power curve was computed in Matlab for each water speed using equation (1) and compared with power values reported by the ABB induction motor drive when the system reached steady-state. Similarly, the expected electrical power was computed using turbine power, generator efficiency and rectifier parameters. Electrical power was also measured using voltage measurements taken across the resistive load. The generator speed was also recorded for each data point and multiplied by $\frac{n_{pto}}{n_{em}N_{gb}}$ to attain an equivalent speed for the modeled river turbine ω_{turb} . The results are shown in Figure 7.

For the dynamic tests, the system is tested first for a step up in water velocity from 0.85 m/sec to 1.15 m/sec. The system is also simulated in Matlab using the function *ode45* to solve equation (3). Both results are shown in Figure 8. Therein, the equivalent turbine speed is shown versus time and the trajectory is shown in the power-speed phase plane. Likewise, the system is then tested and simulated for a step down in water velocity from 1.15 m/sec to 0.85 m/sec, and the results are shown in Figure 9. Good agreement is seen between the simulated (scaled down) river turbine and the emulator hardware result. For the step-up case, some slight differences are noted in the rise time of ω_{turb} and a steady-state error is noted in both experiments at the higher ω_{turb} . Both of these discrepancies may be attributed to assuming a

constant damping coefficient. In particular, although a constant B_m value is assumed, the mechanical damping of the emulator generator is slightly higher at lower speeds than at higher speeds. This is supported by Figure 7 as well; therein, slight differences are seen in the modeled generator power and induction motor power that indicate slightly greater damping at lower speeds than at higher speeds. It is also possible that the generator torque estimator dynamics are playing a minor role; although the estimator is designed to have negligible effect on the dynamics, a minor lag in the generator torque estimate may result in a slightly faster rise time but would not account for the steady-state error.

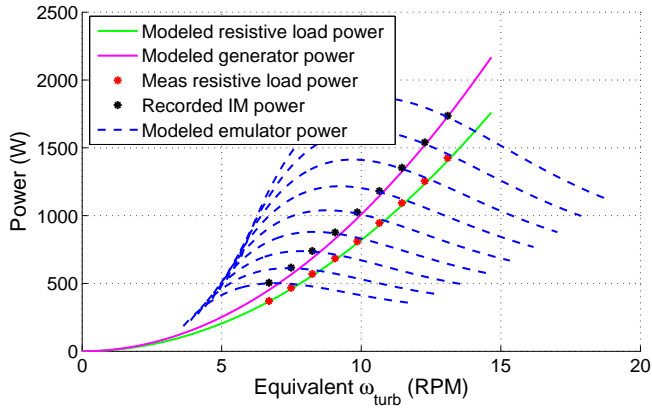


Fig. 7. Steady-state Emulator Power for v_w between 0.7 and 1.1 m/sec

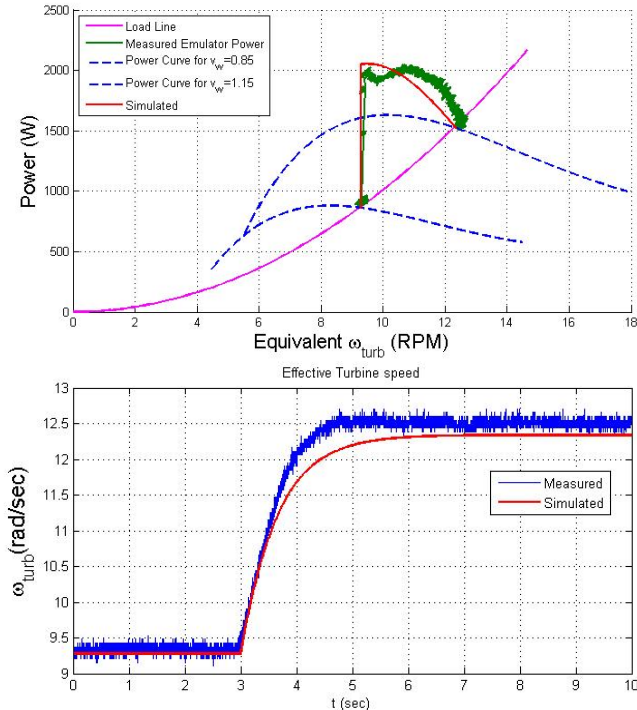


Fig. 8. River Turbine Emulator Dynamic Response v_w stepped from 0.85 to 1.15 m/sec

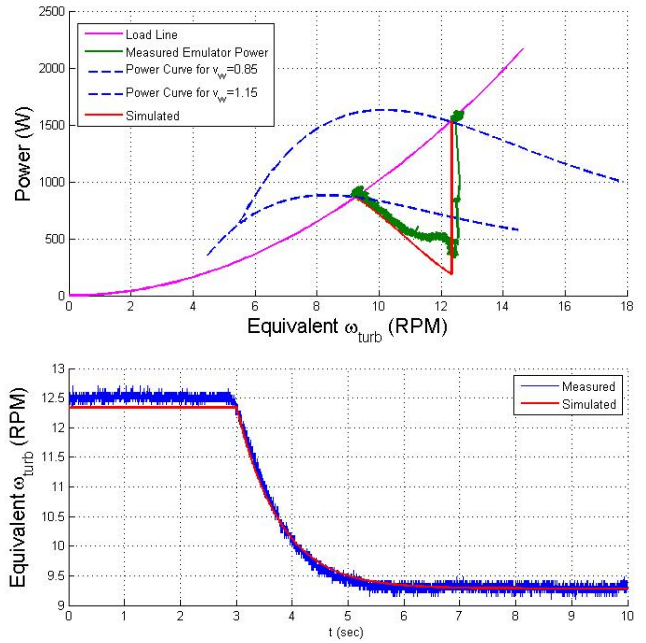


Fig. 9. River Turbine Emulator Dynamic Response v_w stepped from 1.15 to 0.85 m/sec

V. SIMULATION AND HARDWARE RESULTS FOR THE POINT ABSORBER

In this section, simulation and hardware results are presented for a single-body OPT-like point absorber based on the system presented in [8]. Specifically, the excitation and radiation finite impulse response functions are shown in Figures 10 and 11 respectively [8]. Herein, they are resampled at 24 msec timesteps to be in sync with the industrial computer's sampling rate. Additional parameters are given in Table III. Since the Mooring force for the system is particularly small in this model compared to the other forces acting on the buoy, it is neglected, and parameters related to Mooring force are not provided.

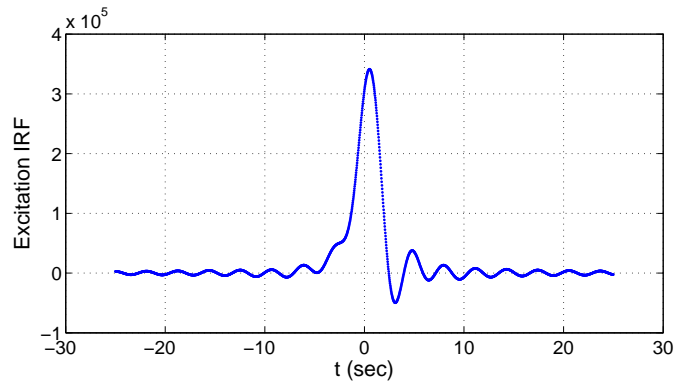


Fig. 10. Single-Body Point Absorber Time-Domain Excitation IRF [8]

The generator is connected through a rectifier with LC output filter to a resistive load. The schematic representation is given in Figure 12.

Two wave profiles are considered. The first involves a

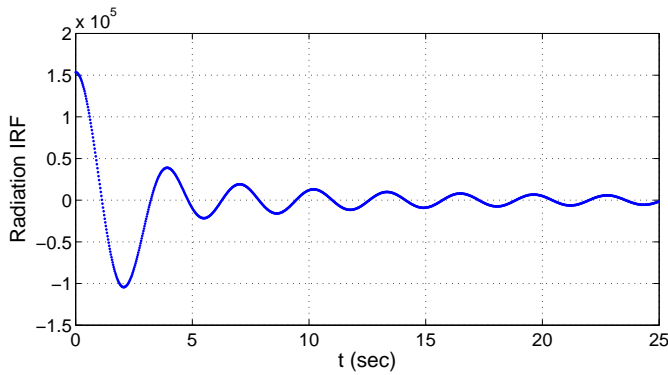


Fig. 11. Single-Body Point Absorber Time-Domain Radiation IRF [8]

TABLE III
POINT ABSORBER EMULATOR EXPERIMENT PARAMETERS

Description	Parameter	Value	Units
Buoy mass	m	251580	kg
PTO viscous damping term	B_{pto}	507690	N-sec/m
Emulator power scale factor	k_{sc}	0.01	unitless
Buoy cross-sectional area	A	95.03	m ²
Gravitational Constant	g	9.81	m/sec ²
Density of seawater	ρ_{sw}	1025	kg/m ³

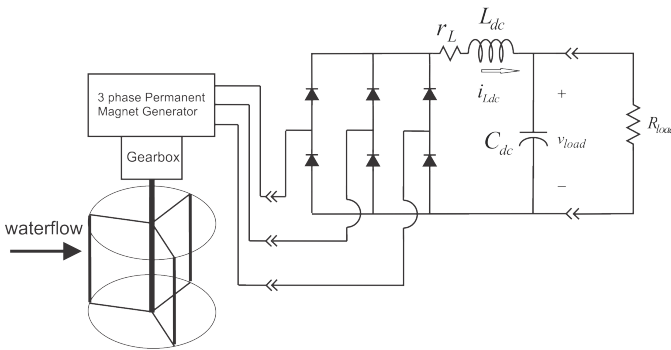


Fig. 12. Schematic representation of point absorber with rectifier and electrical load

regular wave with a wave period of 7 seconds and a peak wave height of 1 meter. Figure 13 displays the wave profile and results of simulation and experiment. The second utilizes a wave profile recorded from a data buoy time-series from Umpqua 46229 in June 2008 [8]. Figure 14 displays the results.

VI. CONCLUSIONS AND FUTURE WORK

Simple methods for emulating a river turbine and a wave energy converter (point absorber) were presented and demonstrated both in simulation and in hardware. Representative models of these invaluable renewable resources have thus been incorporated into the Secure Scalable Microgrid testbed. For the point absorber, a single mass system was modeled and a simple power balance relationship was established for the power take off; subsequent implementations of the point absorber emulator will include a two-body model and will incorporate a detailed model of a hydraulic power take off. Future work will also include the development and testing of

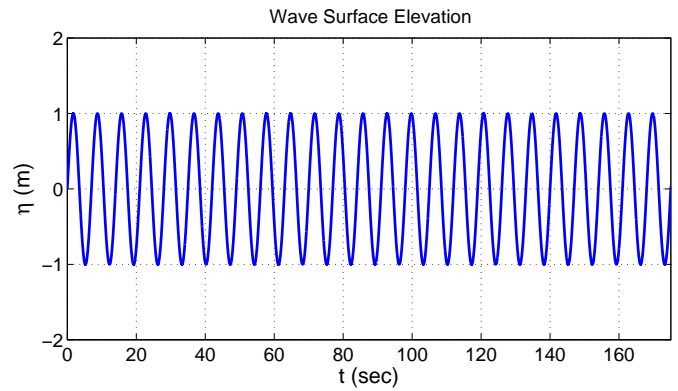


Fig. 13. Simulation and hardware results using a regular wave profile

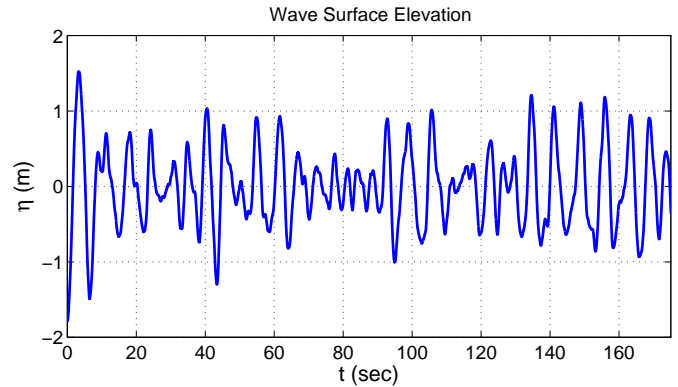


Fig. 14. Simulation and hardware results using an irregular wave profile

control schemes that incorporate hydrokinetic energy sources into power systems that include conventional generation, energy storage and heterogenous loads.

ACKNOWLEDGMENT

Sandia National Laboratories is a multi-program laboratory managed and operated by Sandia Corporation, a wholly owned subsidiary of Lockheed Martin Corporation, for the U.S. Department of Energy's National Nuclear Security Administration under contract DE-AC04-94AL85000.

REFERENCES

- [1] "Mandatory renewable energy target (wikipedia (1-14-2013))." http://en.wikipedia.org/wiki/Mandatory_renewable_energy_target#cite_note-13, 2012.
- [2] "Database of state incentives for renewables and efficiency (dsire)." <http://www.dsireusa.org/rpsdata/index.cfm>, 2012.
- [3] S. McArthur and T. Brekken, "Ocean wave power data generation for grid integration studies," *IEEE Power and Energy Society General Meeting*, July 2010.
- [4] J. Neely, S. Pekarek, S. Glover, J. Finn, O. Wasynczuk, and B. Loop, "An economical diesel engine emulator for micro-grid research," *Speedam Symposium*, June 2012.
- [5] J. Neely, S. Glover, O. Wasynczuk, and B. Loop, "Wind turbine emulation for intelligent microgrid development," *IEEE Cyber-2012 Conference*, May 2012.
- [6] S. Glover, J. Neely, A. Lentine, J. Finn, F. White, P. Foster, O. Wasynczuk, and B. Loop, "Secure scalable microgrid test bed at sandia national laboratories," *IEEE Cyber-2012 Conference*, May 2012.
- [7] M. Barone, T. Griffith, and J. Berg, "Reference model 2: rev0 rotor design," Tech. Rep. SAND2011-9306, Sandia National Laboratories Report, Albuquerque, New Mexico, November 2011.

- [8] K. M. Ruehl, "Time-domain modeling of heaving point absorber wave energy converters, including power take-off and mooring," Master's thesis, Oregon State University, May 19th 2011.
- [9] J. Khan, T. Iqbal, and J. Quaicoe, "Power tracking control challenges in hydrokinetic energy conversion systems," *IEEE Power and Energy Society General Meeting*, July 2010.
- [10] "Matlab the language of technical computing, the mathworks,inc., 3 apple hill drive, natick, ma 01760-2098usa." info@mathworks.com.
- [11] "Labview system design software, national instruments." <http://www.ni.com/labview/>.